ACS Sustainable Chemistry & Engineering

Research Article

pubs.acs.org/journal/ascecg

Green Approach for Augmenting Biocompatibility to Quantum Dots by Extremophilic Polysaccharide Conjugation and Nontoxic Bioimaging

Sreejith Raveendran, Aswathy Ravindran Girija, Sivakumar Balasubramanian, Tomofumi Ukai, Yasuhiko Yoshida, Toru Maekawa, and D. Sakthi Kumar*

Bio-Nano Electronics Research Centre, Graduate School of Interdisciplinary New Science, Toyo University, Kawagoe, Saitama 350-8585, Japan

ABSTRACT: The nanocrystals, so-called quantum dots (QDs), are undisputedly excellent fluorescent markers for imaging and clinical diagnostics. However, their toxicity is always a perturbing issue and remains as the major hindrance for biocompatible imaging and other biomedical applications. Here, we have demonstrated the extraction and application of an extremophilic bacterial polysaccharide, mauran (MR), from a moderately halophilic bacterium called *Halomonas maura* in the stabilization of ZnS:Mn^{2+} QDs for the first time. MR has been employed as a natural polymer for bioconjugation to enhance the cellular acceptance and decrease the cytotoxicity of QDs while being used as a fluorescent marker for imaging purposes. Five nanometer-sized QDs were stabilized using an aqueous MR solution under ambient conditions to yield 10−20 nm-sized nanoparticles. Characterization of MR-QD was performed using UV−vis and fluorescent spectroscopy, TEM, SEM, and FTIR. A cytocompatibility assay revealed that the cellular toxicity of QDs was drastically reduced on MR stabilization. *In vitro* cellular imaging of mouse fibroblast cells and breast adenocarcinoma cells showed that MR-QDs are equally effective as normal QD imaging without imparting any toxicity issues. Thus, it was shown that extremophilic sulfated bacterial polysaccharide, MR, can be successfully used as a novel stabilizing agent for QDs to reduce toxicity and eventually be used as a safe fluorescent agent for *in vitro* imaging.

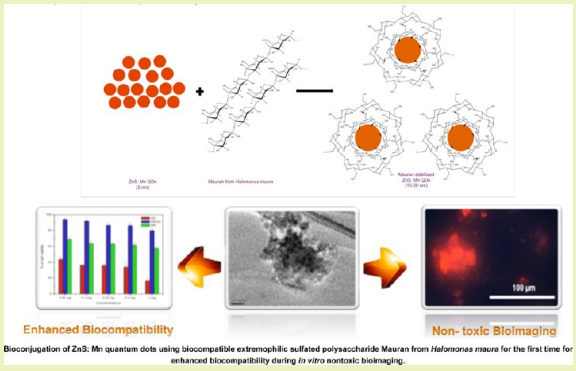

Bioconjugation of ZnS: Mn quantum dots using biocompatible extremophilic sulfated polysaccharide Mauran from *Halomonas maura* for the first time for enhanced biocompatibility during *in vitro* nontoxic bioimaging.

KEYWORDS: *Bacterial polysaccharide, Mauran, Quantum dots, Nanocrystals, Bioimaging, Extremophiles*

INTRODUCTION

Modern nanotechnology plays an indispensable role in the field of pharmaceutical science and medicine for a variety of applications. Nanomaterials in the form of nanocapsules, nanoparticles, nanocrystals, etc. have been widely used in the areas of drug delivery, imaging, cancer therapy, Si-RNA delivery, and biosensors.[1,2] Among nanocrystals, quantum dots (QD) are well known for their photoluminescence and are used as imaging agents for biological tissues.[3] Mainly, they are employed for deep tissue imaging and clinical diagnostic applications in the form of fluorescent markers.[4,5] QDs must be tailored in such a fashion that they can be safely used for live cellular imaging, *in vivo* studies, and cancer diagnostics. However, most available techniques for QD synthesis are either involving toxic chemicals or high temperatures. These methods yield QDs with hydrophobic and water-insoluble properties.[6] Generally QDs are highly toxic, although there are several modes of nontoxic QD fabrication as well as stabilization processes with biocompatible polymers. QDs are either stabilized with a capping agent or conjugated with a biocompatible polymer that can offer excellent biocompatibility and *in vivo* cellular acceptance.[7]

ZnS nanocrystals doped with other metal ions are well studied for their complex photoluminescence mechanisms. Photoluminescence can be attributed to two mechanisms of emission: excitonic and trapped luminescence. In the case of ZnS QDs, trapped emission is observed, which is wide and Stokes shifted.[8] Transition metal-doped QDs are gaining serious attention from material researchers for their excellent semiconductor properties and high luminescence efficiencies.[8,9] Recently, these highly efficient nanocrystals are extensively applied for manufacturing sensors, displays, and lasers.[10] Mn^{2+}-doped ZnS QDs are studied for multifarious applications including cellular imaging, drug delivery, and cancer treatment.[9] Water-soluble ZnS:Mn QDs can be obtained through several methods that involve various chemicals and heat treatment.[8] However, biocompatibilities of the so-formed nanocrystals are still a matter of concern during various applications including *in vivo* studies.

Special Issue: Sustainable Nanotechnology 2013

Received: January 3, 2014
Revised: March 3, 2014
Published: April 4, 2014

MR is an extremophilic bacterial polysaccharide isolated from a moderately halophilic bacterium, *Halomonas maura*. It is a physiologically versatile bacterium with both ecological and biotechnological interests.[11] MR has been well established as an interesting sulfated heteropolysaccharide with exceptionally good physicochemical properties and bioactivities. It offers numerous industrial applications because MR is capable of emulsifying several types of oil more efficiently than some chemical surfactants.[12] Owing to the high viscoelasticity and pseudoplasticity, MR is reported to be a good candidate for cosmetics, food, and pharmaceutical applications. Apart from its industrial and pharmaceutical applications, MR plays a critical role as an immunomodulator and offers antiproliferative effects against cancer cells.[11] More recently, MR was recognized as an ideal biomaterial in nanotechnology for the synthesis of nanoparticles for drug delivery, cancer chemotherapy, and bioimaging.[1] Furthermore, MR-based nanofiber scaffolds were demonstrated to be excellent meshworks for tissue engineering applications because they showed enhanced cell adhesion and proliferation under *in vitro* cell culture conditions.[13] Studies show that MR is a novel biomaterial that can be successfully employed for various nanotechnological applications in the field of biomedicine and material science without compromising the matter of biocompatibility.

In the present study, we stabilize ZnS:Mn QDs by bioconjugating with a versatile extremophilic exopolysaccharide, MR, for enhanced biocompatibility and cellular acceptance during *in vitro* live cellular imaging.

EXPERIMENTAL SECTION

Bacterial Strain and Mammalian Cell Line. Moderately halophilic bacteria, *H. maura* (ATCC 7000995), was procured and propagated as per the instructions provided in the product information sheet from ATCC. Mouse connective tissue (L929) fibroblast cells and breast adenocarcinoma cells (MCF7) were purchased from the Riken Bio Resource Center, Japan, for conducting biocompatibility and bioimaging studies, respectively.

Chemicals. Zinc acetate, manganese sulfate, and sodium sulfide nonahydrate were purchased from Kanto Chemicals, Japan. Dulbecco's modified Eagle's medium (DMEM) used for cell culture studies was purchased from Sigma-Aldrich. Fetal bovine serum (FBS), penicillin, streptomycin, amphotericin B, and alamar blue were purchased from Gibco, Invitrogen, U.S.A. All other chemicals used were of reagent grade.

MR Production and Extraction. *H. maura* was grown in MY medium as mentioned elsewhere.[1] MR was extracted and purified to remove metal salts and other impurities via dialysis; later, it was subjected to lyophilization.[1] Powdered MR was used for QD stabilization studies.

Synthesis of ZnS:Mn QDs. ZnS:Mn QDs were prepared as mentioned elsewhere.[9] Briefly, 0.1 M Zn $(CH_3COO)_2$ solution was prepared in 10 mL of deionized water and purged with N_2 for 10 min. A 0.01 M $MnSO_4{\cdot}H_2O$ solution was also prepared in deionized water, and 1 mL was added dropwise to the Zn $(CH_3COO)_2$ solution under constant stirring for 10 min. Ten milliliters of 0.1 M $Na_2S{\cdot}9H_2O$ solution was added slowly to the above mixture, with continued stirring for another 30 min. Formation of ZnS:Mn QDs were confirmed by observing the orange-red fluorescence under UV illumination around 365 nm. The QD solution prepared was washed with deionized water by centrifugation and dried using a lyophilizer to obtain a fine powder of ZnS:Mn QDs.

Synthesis of MR Conjugated QDs (MR-QD). MR-QDs were prepared using powdered MR and ZnS:Mn QDs. MR was dissolved in deionized water to obtain a concentration of 2 mg/mL. The MR solution was stirred continuously for 30 min to obtain a homogeneous suspension. A total of 0.5 mg of ZnS:Mn QDs was weighed and suspended in 1 mL of deionized water. This 1 mL solution of ZnS:Mn QD suspension was added dropwise to the MR solution under constant stirring. The MR-QD solution was centrifuged to collect the pellet and suspended in 1 mL of deionized water for characterization and *in vitro* cell culture studies.

Characterization of MR-QD. Spectroscopic characterization of MR-QD was performed using UV-vis spectrophotometry and fluorescence spectroscopy. UV−vis spectra of MR-QD nanoparticles were measured using a Beckman Coulter Life Sciences UV/vis spectrophotometer DU730 and compared with individual spectra of MR and ZnS:Mn QD. Fluorescence emission of MR-QD was observed and measured using a Hitachi F-4500 fluorescence spectrophotometer at an excitation wavelength of 360 nm. Morphological characterization of MR-QD was performed using electron micrographic observations. TEM images of MR-QD were recorded using JEOL, JEM-2200FS. One drop of MR-QD suspension was placed on a carbon-coated copper grid after hydrophilizing the grid for 30 s in a TEM grid hydrophilizer (JEOL DATUM, HDT-400) and dried thoroughly. Nanoparticles were observed using TEM under 200 kV, and images were recorded. Simultaneously, detection of various constituent elements present in the MR-QD was performed using energy dispersive X-ray spectroscopy (EDS) (JED-2300T). Surface characteristics of the bioconjugated QD nanoparticles were analyzed using SEM (JEOL, JSM-7400F). Vacuum-dried samples on silica substrates were sputter coated with Pt on a high-resolution sputter coater (Hitachi, E-1030, Ion sputter) before SEM observation. FTIR spectra were recorded for MR-QD, MR, and QD and compared with each other. The sample was mixed with 200 mg of dry KBr pellets and ground thoroughly, and the mixture was pressed into a 16 mm diameter mold to prepare pellets for FTIR analysis. Infrared spectra were recorded (PerkinElmer, U.S.A.) with a resolution of 4 cm^{-1} in the region of 4000−400 cm^{-1}.

***In Vitro* Cytotoxicity and Cell Imaging Studies.** *Cell Culture.* L929, mouse fibroblast cell line, and MCF7, breast cancer cell lines, were used for testing the *in vitro* cytotoxicity and imaging studies using MR-QD nanoparticles, respectively. L929 cells and MCF7 cells were cultured and maintained separately using DMEM, supplemented with 10% of FBS at 37 °C in a 5% CO_2 atmosphere. Cells were subcultured after attaining confluent growth and seeded into 96 well plates for testing cytotoxicity and 33 mm glass base dish for imaging on the order of 5000−8000 cells/well and 3×10^4 to 6×10^4 cells/plate, respectively.

Alamar Blue Assay. Alamar blue assay was performed to detect the percentage of cell viability on the basis of the natural reducing power of the viable cells to convert resazurin to a fluorescent molecule, resorufin. Quantification of the cell viability in the presence of MR-QD and QD nanocrystals will directly measure the cytotoxicity caused by these materials. Alamar blue assay was performed as per the standard protocol. L929 cells were grown in 96 well plates for 24 h and treated with varying concentrations of MR-QD nanoparticles (50, 100, 250, 500, and 1000 μg/mL) to check its biocompatibility toward normal cells. Plates were incubated at 37 °C for 24 h under a 5% CO_2 atmosphere. At the end of incubation, 10% of alamar blue dye was added to each well and incubated for 4 h. Afterward, fluorescence was measured at 580−610 nm using a multidetection microplate reader (Dainippon Sumitomo Pharma, Powerscan HT). The experiment was conducted in triplicate, and results were plotted by deducing the mean ± SD.

Cellular Uptake Studies: Flow Cytometry. L929 cells treated with MR-QD nanocrystals were employed for confirming the cellular uptake and to support the cytotoxicity assay. Flow cytometry analysis of fluorescent MR-QD nanoparticles was performed using two set of samples: freshly prepared MR-QD nanocrystals and 3 month old refrigerated MR-QD nanocrystals (to evaluate the photo stability under storage conditions). L929 cells grown in tissue culture flasks containing DMEM medium were incubated for 24−48 h to obtain a confluent growth. A total of 500 μL of MR-QD-new and MR-QD-old samples were added to the culture flasks and incubated at 37 °C for 24 h under a 5% CO_2 atmosphere. After incubation, unabsorbed nanocrystals were washed using 1X PBS solution. Approximately 1

$\times 10^7$ cells were harvested separately from each plate and fixed with a 3% formaldehyde solution for 20 min. At the end of incubation, cells were centrifuged at 3500 rpm for 3 min, and pellets were collected. Cells were then washed and permeabilized using 70% ice cold ethanol for 10 min at −20 °C. Pellets were collected and suspended in PBS solution for flow cytometry analysis. Fluorescence intensity emitted from the cells were detected using a JSAN cell sorter from Bay Biosciences, Japan, with a laser with a 402−446 nm wavelength. Data was analyzed using JSAN App San software, and graphs were presented.

***In Vitro* Cellular Imaging.** MCF7 breast adenocarcinoma cells were used for conducting *in vitro* cellular imaging. MCF7 cells were seeded into a 33 mm glass base dish on the order of 3×10^4 to 6×10^4 cells/plate. Cells were incubated at 37 °C for 24 h under a 5% CO_2 atmosphere for obtaining confluent growth. A total of 100 μL of MR-QD nanoparticles were added to the cells and incubated for another 24 h. This is to observe the passive absorption of MR-QD particles by the cancer cells. At the end of incubation, unbound and unabsorbed nanocrystals were washed using sterile 1X PBS. Prior to imaging, 300 μL of PBS was added to the cells to prevent desiccation. Passive absorption of MR-QD nanoparticles by MCF7 cells was confirmed by imaging the cells using a phase contrast epifluorescent microscope (Nikon Eclipse, TE2000-U inverted microscope with twin CCD cameras) with 40X oil immersion objectives. Orange-red fluorescence of MR-QD nanoparticles was observed using band-pass excitation and emission filters, BP 365/10 nm (excitation) and 400 nm (emission), with 400 nm dichromatic mirror.

RESULTS AND DISCUSSION

Synthesis and Characterization of MR-QD. *H. maura* was grown for MR production, and MR was extracted using a cold ethanol extraction method. Lyophilized MR powder was used for the experiment. Figure 1 shows the SEM image of *H. maura* showing the MR accumulation surrounding the cell wall of the bacteria. Application of MR as a passivation agent for increasing the biocompatibility of QDs makes it ideal for biological applications. The property of QDs to emit fluorescent light is being exploited popularly for clinical diagnostic applications in the form of imaging biomarkers. The toxicity of ZnS:Mn QDs hampers its application in living tissues; it has been overcome by stabilizing with an extremophilic bacterial polysaccharide MR. Figure 2 is a schematic representation of the process of stabilization of ZnS:Mn QDs using MR for making a biocompatible safe imaging agent. QDs of 5 nm in size have been treated with MR solution with a concentration of 2 mg/mL under continuous magnetic stirring to yield hybrid nanocrystals of MR-ZnS:Mn QDs with sizes of 10−20 nm. The polyanionic nature of the MR greatly contributes to the hybrid formation of MR-ZnS:Mn clusters. This could be due to the ionic cross-linking of anionic functionalities of MR (SO_4^{2-} and COO^-) and the cationic counterpart of QDs. As reported previously, MR possesses an excellent metal-binding property, which was used to remove toxic heavy metal contaminants from water.[14]

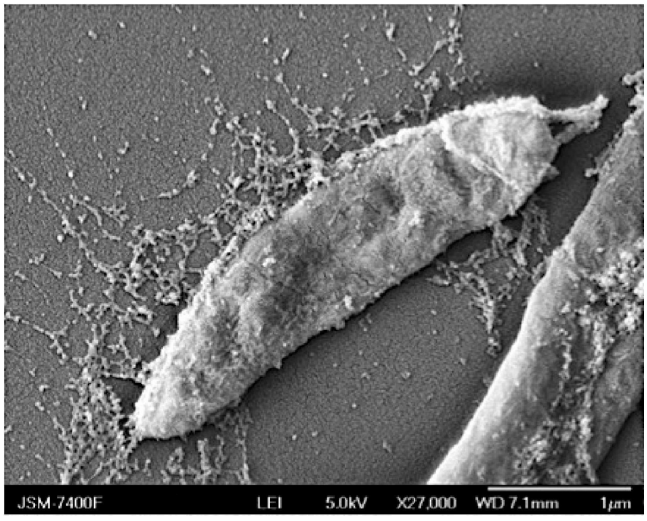

Figure 1. SEM micrograph of *Halomonas maura* showing the exopolysaccharide, MR, covering the cell wall.

Preliminary confirmation of the MR-QD hybrid nanocrystals formation was by illuminating the sample under UV to observe orange-red fluorescence. Two sets of MR-QD samples were analyzed for the characterization. A freshly prepared sample and a sample stored at 4 °C for 3 months were used for analysis. This is to show the photo stability of the MR-QD nanocrystals under storage conditions. Figure 3 shows the UV−vis spectra of QD, MR, MR-QD-new and MR-QD-old samples. The absorption peak of the ZnS:Mn QDs was observed at 320 nm, which was slightly shifted to 325 nm showing successful stabilization of MR on QDs. The red shift in the absorption peak was due to an increase in the size of the nanoparticles on MR stabilization. Another prominent peak observed a QD spectrum at 218 nm, which can be due to the ZnS component of the ZnS:Mn QDs.[8]

The PL spectra of the Mn^{2+}-doped ZnS QDs have different characteristic emissions according to the amount of Mn^{2+} doping.[8,15] It was already reported that the ZnS:Mn QDs emit two different wavelengths: blue emission and orange emission. Generally, Mn^{2+}-doped QDs have a typical orange-red bulk emission at 580 nm on UV excitation. Murugadoss et al. have reported that when the concentration of the Mn^{2+} ions increases, the blue emission will be quenched, and slowly the orange-red fluorescent emission will become prominent.[8] According to the PL spectra shown in Figure 4, the orange-red emission was observed in the range of 580 nm. This shows that the amount of Mn^{2+} doping is in the range of 0.5−4%. For ZnS:Mn QDs bioconjugation with MR, the characteristic orange-red emission was maintained, although the intensity of the fluorescence was significantly reduced. This can be due to masking of the direct luminescence shown by the QD crystals. However, it is evident that the stabilization of ZnS:Mn QDs using MR polysaccharide does not have a serious effect on the fluorescence emission in comparison to bare QDs, although there is some quenching effect. Similarly, a slight difference in the intensity of the emission was observed in the case of the new set and old set of the MR-QD samples. However, it is relevant that the particles were still maintaining photo stability to show a pertinent emission at 580 nm even after 3 months of storage under 4 °C.

Figure 5A depicts the TEM image of the bare QDs with a size around 5 nm. The image clearly shows the crystalline pattern of the ZnS:Mn QDs, which on stabilization with MR is slightly masked due to a coating provided by the MR polysaccharide. Figure 5B and C shows a cluster of MR-QD nanocrystals, whereas Figure 5D depicts the individual nanocrystals with complete coating of MR over the surface of QDs. Microscopic identification was further confirmed using spectroscopic analysis using TEM-EDS. Figure 6A shows the EDS spectra of MR-QD nanocrystals observed using TEM. A peak corresponding to S in the spectra shows the sulfate functionalization of the nanoparticles. This ensures the

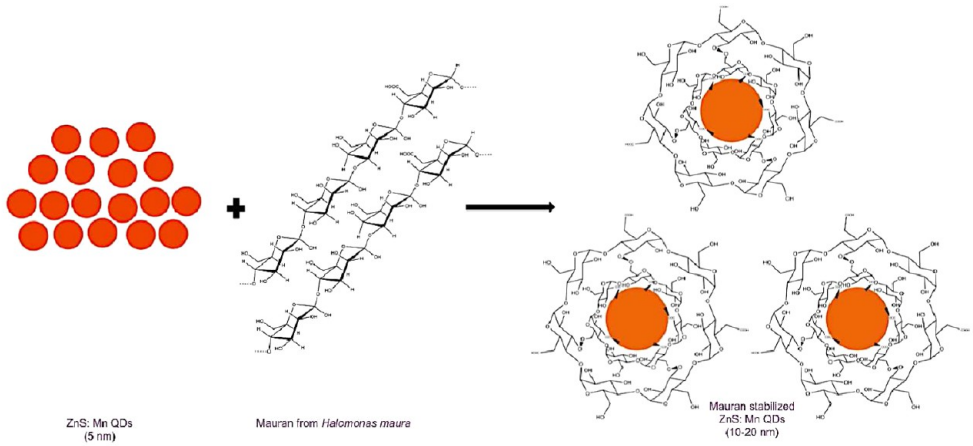

Figure 2. Schematic representation of QD stabilization with extremophilic sulfated polysaccharide, mauran, from *Halomonas maura*.

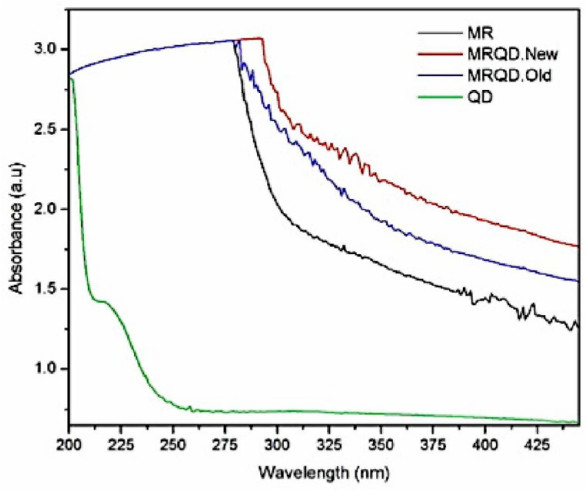

Figure 3. UV−vis spectra.

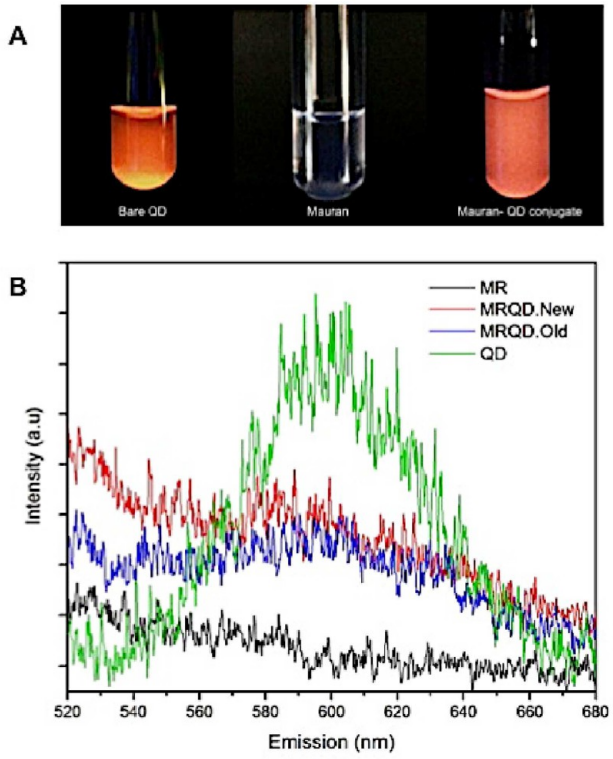

Figure 4. (A) UV illuminated images of bare QDs, mauran, and MR-QDs. (B) Photoluminescence spectra.

successful conjugation of MR on the surface of the QDs. Geddie and Sutherland have demonstrated that anionic polysaccharides prefer to bind cations on the whole with large ionic radii.[16] The polyanionic nature of the MR molecules enhances the rate of attraction for cationic molecules, including various heavy metals. This property of MR was previous explained by Arias et al.,[14] where heavy metal uptake studies were performed using various metal salt solutions containing Ag^{+}, Co^{2+}, Cu^{2+}, Mn^{2+}, Ni^{2+}, Pb^{2+}, and Zn^{2+}. The metal binding property of MR irrespective of the amount of deacetylation shows the possibility of stabilization of several metal nanocrystals like ZnS:Mn QDs. Furthermore, morphological and surface characteristics of MR-QDs were analyzed using SEM. Figure 6B and C shows the SEM micrographs of MR-QD nanoclusters under different magnifications, respectively. Electron micrographic studies reveal that the bioconjugation of QDs using MR can either result in agglomeration or formation of individual nanoclusters due to high surface charge density of MR. A higher degree of sulfation and $COOH^{-}$ groups from the constituent glucuronic acid residues makes MR highly polyanionic.[14] Also, the acetyl groups present in MR can bring more positively charged ions to the vicinity of binding site, thus allowing a stronger binding. As the number of binding sites per unit molecule increases, the chances of attracting positively charged crystals to a unit molecule of polysaccharide also increases, resulting in agglomerates or nanoclusters.

FTIR analysis demonstrates and compares the structures of nanoparticles with the help of characteristic bonds present in the MR, QD, and MR-QD formed. Figure 7 shows the characteristic peaks in the FTIR spectra of the tested samples. Curve 1 depicts the IR spectrum of MR-QD, which can be precisely compared with the spectrum of QD (Curve 2) and the spectrum of MR (Curve 3). The two major peaks observed around 3854−3430 and 2923 cm^{-1} correspond to O−H and C−H stretching of the MR coating over the nanocrystals, respectively, which is common to all polysaccharides.[17,18] Strong absorption bands at 1741 and 1631 cm^{-1} can be due to the carboxylic ester (C═O) form and carboxylate anionic (COO−) form present in the uronic acid residues of the MR,

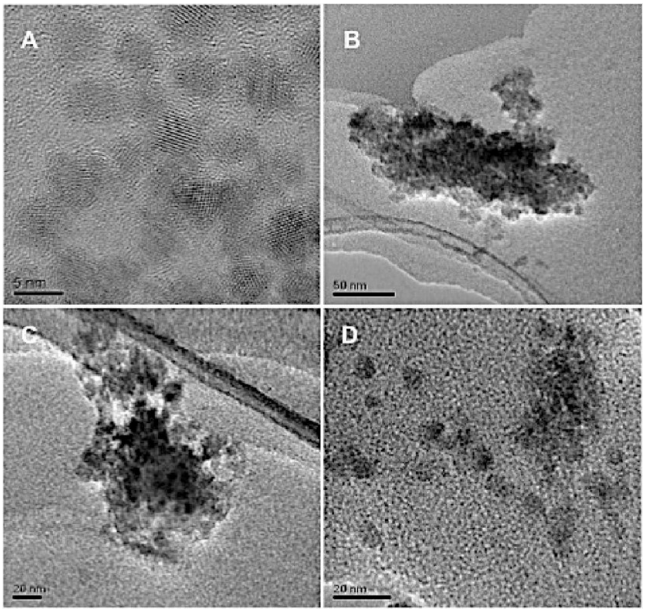

Figure 5. TEM micrographs showing (A) ZnS:Mn QDs, (B and C) clusters of MR-QDs, and (D) individual MR-QD particles.

respectively. The presence of a characteristic sulfate group of MR in MR-QD nanoparticles was confirmed with the stretching vibration observed at 1261 cm^{-1}.[1,13] Similarly, another important vibration observed at 1101 cm^{-1} depicts the C−C stretching of the pyranoid ring of the polysaccharide residues. The prominent absorption peak shown at 618 cm^{-1} corresponds to the sulfide bonding of the ZnS nanocrystals.[19]

***In Vitro* Cellular Uptake and Imaging Studies.** Results of cytotoxicity studies performed using various concentrations of MR-QD, QD, and MR are shown in Figure 8. As mentioned earlier, the toxicity of QDs has to be reduced to make it an ideal agent for bioimaging purposes. Bare ZnS:Mn QDs were found to be highly toxic when five different concentrations were treated with mouse fibroblast cell lines. The lowest concentration of bare QDs treated was 0.05 mg, which showed only ∼44% cell viability. On stabilization using MR, it was observed that the percentage of viability drastically increased. The highest treated concentration of MR-QD was 1 mg, and it successfully showed viability around 80%. In one of our previous papers, we have demonstrated the application of MR-chitosan nanoparticles for sustained drug delivery, cancer chemotherapy, and bioimaging.[1]

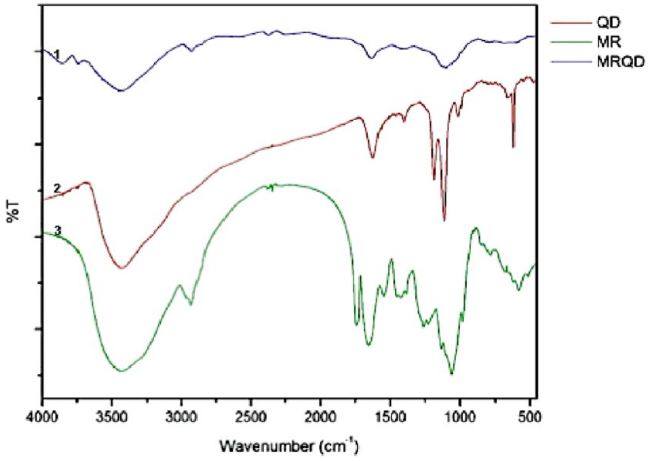

Figure 7. FTIR spectra.

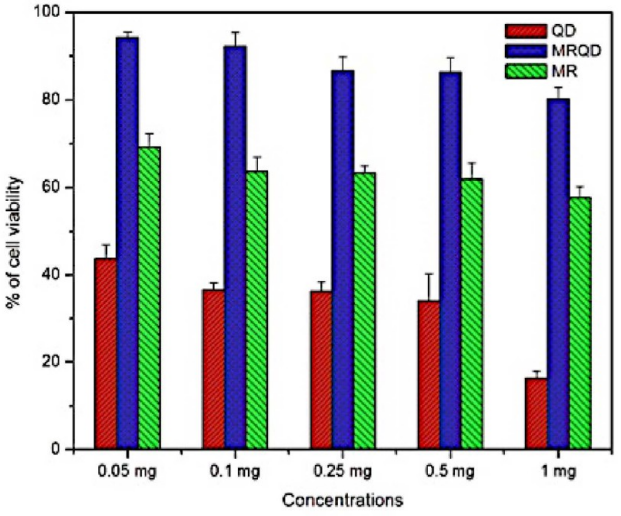

Figure 8. *In vitro* cytotoxicity using L929 mouse fibroblast cells.

It was shown that fluorescently tagged MR in the form of nanoparticles were highly biocompatible for bioimaging. Although bare MR polysaccharide showed a slight dose-dependent cytotoxicity at higher concentrations toward L929 cells, the percentage of viability was enhanced when it was given in the form of MR-QD nanoparticles. This can be attributed to the size-dependent acceptance of particles by the

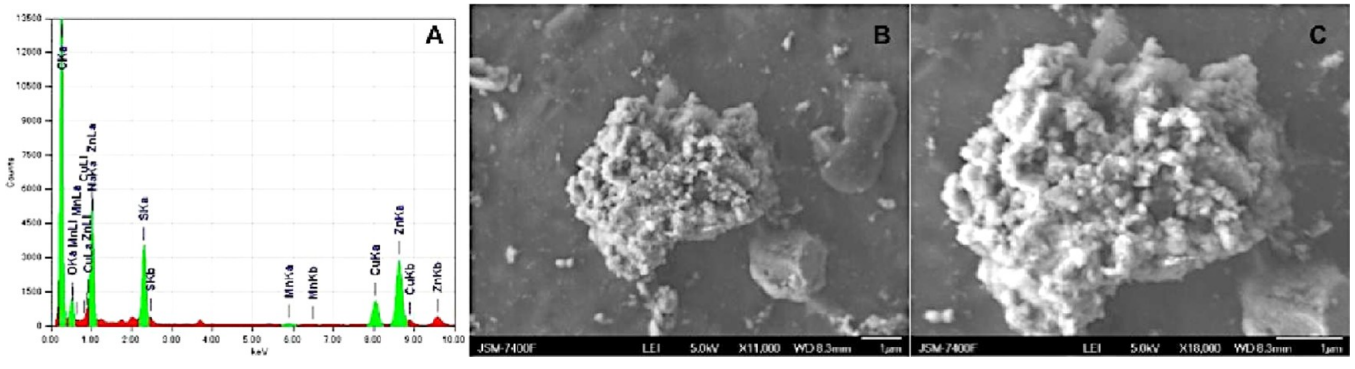

Figure 6. (A) TEM- EDS spectrum showing the constitutive elements detected in MR-QD nanocrystals. (B and C) SEM micrographs showing clusters of MR-QDs under different magnifications.

dx.doi.org/10.1021/sc500002g | *ACS Sustainable Chem. Eng.* 2014, 2, 1551−1558

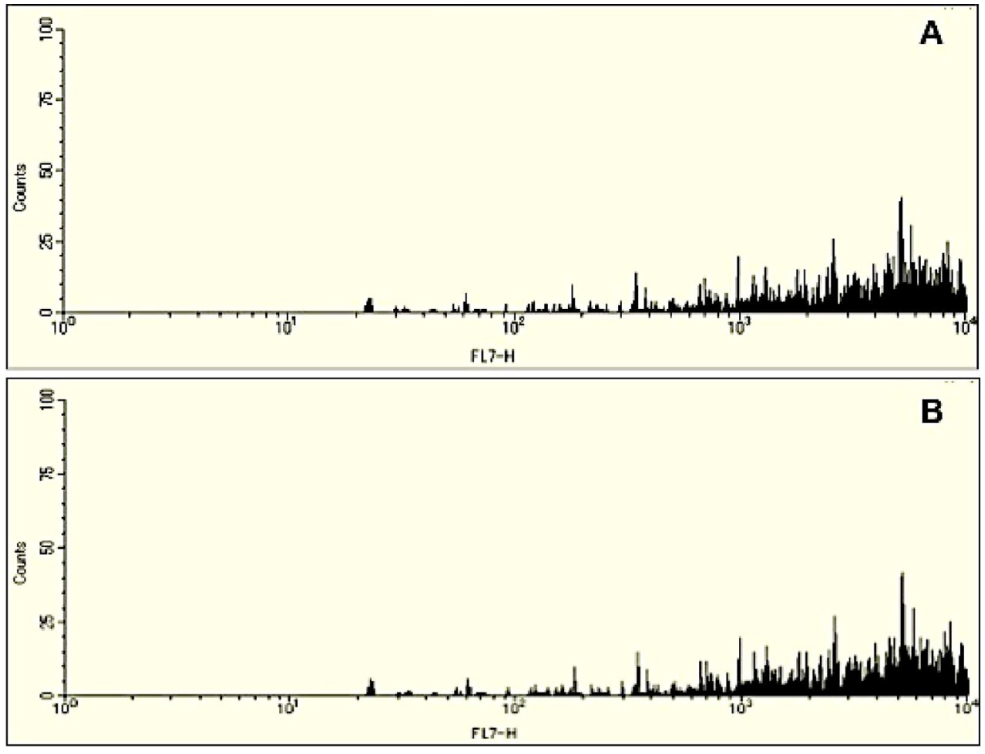

Figure 9. Flow cytometry spectra showing the uptake of fluorescent MR-QD particles by L929 cells: (A) MR-QD-new set, (B) MR-QD-old set.

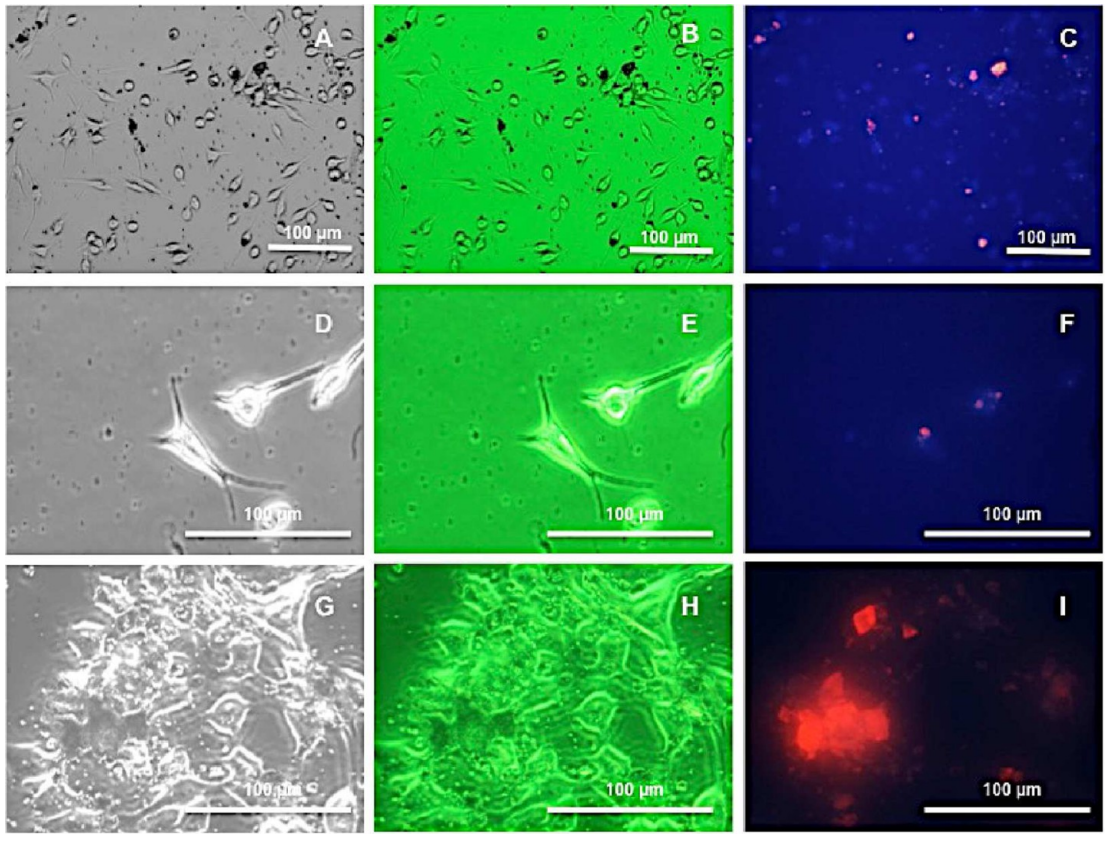

Figure 10. Phase contrast and epifluorescent imaging of MR-QD-treated L929 cells and MCF7 cells: (A and D) Bright field image of L929, (B and E) phase contrast image of L929, (C and F) epifluorescent image of L929, (G) Bright field image of MCF7, (H) phase contrast image of MCF7, and (I) epifluorescent image of MCF7.

mammalian cells. Unlike other bacterial polysaccharides, mauran has a high degree of sulfation with high molecular weight that plays a vital role in deciding its biological properties.[14,20,21]

dx.doi.org/10.1021/sc500002g | ACS Sustainable Chem. Eng. 2014, 2, 1551−1558

The amount of cellular uptake of fluorescent MR-QDs were analyzed using flow cytometry analysis. Figure 9 shows the flow cytometry fluorescence distribution data of the L929 cells treated with MR-QDs. Figure 9A depicts the new set of MR-QD and B shows the old set. The fluorescence distribution was found to be uniform in both the cases. Approximately 10^3-10^4 cells were showing fluorescence due to absorption of MR-QD nanoparticles. Thus, it supplements the cytotoxicity result. Three-fourths of the cells used out of 10^7 cells were found to be fluorescently labeled using MR-QD nanoparticles efficiently and safely.

MCF7 breast adenocarcinoma cells and L929 cells were used as two test systems to establish the bioimaging mechanism of MR-QD nanocrystals. Leaky vasculatures of the cancer cells are advantageous over normal cells for nanoparticles to undergo passive transfer and enhanced uptake. On the basis of the natural concentration gradient, the particles will be entering inside the cells, and either they accumulate in cell organelles or they may get flushed out during cellular metabolism. Here, MR-QDs were treated with MCF7 cells and L929 cells for 24 h to allow sufficient cellular uptake via passive mode. Figure 10 shows the bright field, phase contrast, and fluorescent images of L929 and MCF7. The bright orange-red fluorescence observed within the cells in Figure 10C, F, and I corresponds to the MR-QD nanoparticles absorbed by the cells during incubation. Fluorescent images suggest that the cancer cells have more affinity for MR-QD nanoparticles, and they tend to accumulate within the cells. Thus, the stabilization of ZnS:Mn QDs using MR is highly successful in imparting a biocompatible and safe mode of cellular imaging under *in vitro* conditions.

CONCLUSIONS

In summary, we have designed and developed a biocompatible fluorescent nanoparticle by stabilizing ZnS:Mn QDs using extremophilic bacterial polysaccharide, MR, for the first time. Characterization of MR-QD suggested that effective modification of 5 nm-sized nanocrystals into 10 nm-sized nanoparticles with a coating of MR over the surface of QDs occurred. A cytotoxicity assay revealed that MR-QD has excellent biocompatibility compared to bare QDs, which was having limitations in biological applications previously. Here, it is well explained that coating of ZnS:Mn QDs with MR polysaccharide up to the highest test concentration was found to be safe for live cellular imaging. On successful bioconjugation of MR into QDs, we have demonstrated the possibility of introducing novel biological polymers from extremophilic environments to nanotechnology for biomedical applications. Cellular acceptance and their nontoxic nature facilitates the application of MR-QDs as excellent biomarker agents for imaging mammalian cells, tumors, and cancers. Active targeting of these nanocrystals could enhance the cellular binding as well as uptake, which can facilitate cancer diagnosis and treatment. Present findings will be essential for developing various systems with applications beyond *in vitro* imaging by modifying the MR-QDs with targeting moieties for site-specific delivery and *in vivo* imaging.

AUTHOR INFORMATION

Corresponding Author

*Tel: +81 49 239 1375. Fax: +81 49 234 2502. E-mail: sakthi@toyo.jp.

Notes

The authors declare no competing financial interest.

ACKNOWLEDGMENTS

Sreejith Raveendran acknowledges the Ministry of Education, Culture, Sports, Science and Technology (MEXT), Japan, for financial support under the Monbukagakusho fellowship. Also, part of this study has been supported by a grant from the Programme of the Strategic Research Foundation at Private Universities, S1101017, organized by MEXT, Japan, since April 2012.

REFERENCES

(1) Raveendran, S.; Poulose, A. C.; Yoshida, Y.; Maekawa, T.; Kumar, S. Bacterial exopolysaccharide based nanoparticles for sustained drug delivery, cancer chemotherapy and bioimaging. *Carbohydr. Polym.* **2013**, *91*, 22.

(2) Raveendran, S.; Yoshida, Y.; Maekawa, T.; Kumar, S. Pharmaceutically versatile sulfated polysaccharide based bionano platforms. *Nanomedicine* **2013**, *9*, 605.

(3) Aswathy, R. G.; Yoshida, Y.; Maekawa, T.; Kumar, S. Near-infrared quantum dots for deep tissue imaging. *Anal. Bional. Chem.* **2010**, *397*, 1417.

(4) Parveen, S.; Misra, R.; Sahoo, S. K. Nanoparticles: A boon to drug delivery, therapeutics, diagnostics and imaging. *Nanomedicine* **2012**, *8*, 147.

(5) Smith, A. M.; Duan, H.; Mohs, A. M.; Nie, S. Bioconjugated quantum dots for *in vivo* molecular and cellular imaging. *Adv. Drug Delivery Rev.* **2008**, *60*, 1226.

(6) Patra, M. K.; Manoth, M.; Singh, V. K.; Gowd, G. S.; Choundhry, V. S.; Vadera, S. R.; Kumar, N. Synthesis of stable dispersion of ZnO quantum dots in aqueous medium showing visible emission from bluish green to yellow. *J. Lumin.* **2009**, *129*, 320.

(7) Peng, H.; Zhang, L.; Soeller, C.; Travas- Sejdic, J. Preparation of water-soluble CdTe/CdS core/shell quantum dots with enhanced photostability. *J. Lumin.* **2007**, *127*, 721.

(8) Murugadoss, G.; Rajamannam, B.; Ramasamy, V. Synthesis, characterization and optical properties of water-soluble ZnS:Mn^{2+} nanoparticles. *J. Lumin.* **2010**, *130*, 2032.

(9) Aswathy, R. G.; Sivakumar, B.; Brahatheswaran, D.; Raveendran, S.; Ukai, T.; Fukuda, T.; Yoshida, Y.; Maekawa, T.; Kumar, S. D. Multifunctional biocompatible fluorescent carboxymethyl cellulose nanoparticles. *J. Biomater. Nanobiotechnol.* **2012**, *3*, 254.

(10) Bhargawa, R. N. Doped nanocrystalline materials – Physics and applications. *J. Lumin.* **1996**, *70*, 85.

(11) Llamas, I.; del Moral, A.; Martinez-Checa, F.; Arco, Y.; Arias, S.; Quesada, E. *Halomonas maura* is a physiologically versatile bacterium of both ecological and biotechnological interest. *Antonie van Leeuwenhoek* **2006**, *89*, 395.

(12) Bouchotroch, S.; Quesada, E.; Izquierdo, I.; Rodríguez, M.; Béjar, V. Bacterial exopolysaccharides produced by newly discovered bacteria belonging to the genus Halomonas, isolated from hypersaline habitats in Morocco. *J. Ind. Microbiol Biotechnol.* **2000**, *24*, 374.

(13) Raveendran, S.; Dhandayuthapani, B.; Nagaoka, Y.; Yoshida, Y.; Maekawa, T.; Kumar, S. D. Biocompatible nanofibers based on extremophilic bacterial polysaccharide from *Halomonas maura*. *Carbohydr. Polym.* **2013**, *92*, 1225.

(14) Arias, S.; Moral, A. D.; Ferrer, M. R.; Tallon, R.; Quesada, E.; Bejar, V. Mauran, an exopolysaccharide produced by the halophilic bacterium *Halomonas maura*, with a novel composition and interesting properties for biotechnology. *Extremophiles* **2003**, *7*, 319.

(15) Geske, M.; Murias, M.; Balan, L.; Medjahdi, G.; Korczynski, J.; Moritz, M.; Lulek, J.; Schneider, R. Folic acid-conjugated core/shell ZnS:Mn/ZnS quantum dots as targeted probes for two photon fluorescence imaging of cancer cells. *Acta Biomater.* **2011**, *7*, 1327.

(16) Geddie, J. L.; Sutherland, I. W. Uptake of metals by bacterial polysaccharides. *J. Appl. Bacteriol.* **1993**, *74*, 467.

(17) Dev, A.; Binulal, N. S.; Anitha, A.; Nair, S. V.; Furuike, T.; Tamura, H.; Jayakumar, R. Preparation of poly(lactic acid)/CH nanoparticles for anti-HIV drug delivery applications. *Carbohydr. Polym.* **2010**, *80*, 833.

(18) Gomes-Ordonez, E.; Ruperez, P. FTIR-ATR spectroscopy as a tool for polysaccharide identification in edible brown and red seaweeds. *Food Hydrocolloids* **2011**, *25*, 1514.
(19) Rema Devi, B. S.; Raveendran, R.; Vaidyan, A. V. Synthesis and characterization of Mn^{2+} doped ZnS nanoparticles. *Pramana* **2007**, *68*, 679.
(20) Bouchotroch, S.; Quesada, E.; Del Moral, A.; Llamas, I.; Bejar, V. *Halomonas maura* sp. nov., a new moderately halophilic, exopolysaccharide-producing bacteria. *Int. J. Syst. Evol. Microbiol.* **2001**, *51*, 1625.
(21) Raveendran, S.; Palaninathan, V.; Chauhan, N.; Sakamoto, Y.; Yoshida, Y.; Maekawa, T.; Mohanan, P. V.; Kumar, D. S. *In vitro* evaluation of antioxidant defense mechanism and hemocompatibility of mauran. *Carbohydr. Polym.* **2013**, *98*, 108.